Bulletin of Environment, Pharmacology and Life Sciences
Bull. Env. Pharmacol. Life Sci., Vol 12 [4] March 2023 : 161-171

Online ISSN 2277-1808
Journal's URL:http://www.bepls.com
CODEN: BEPLAD

ORIGINAL ARTICLE **OPEN ACCESS**

Studies on Silver Nanoparticle Preparation, Synthesis, and Anti-Bacterial Activity of *Rivea hypocrateriformis* (Desr.) Choisy

M.Mahesh*[1]G.Prabhakar[2] and P. Kamalakar[3]
1*and 3, Department of Botany, University College of Science, Osmania University, Hyderabad, Telangana -500 007.
2 Sri Gp Avens Life Sciences, Pvt Ltd, AIC-CCMB, Medical Biotechnology complex, Annex-2, Habsiguda, IDA, Uppal, Hyderabad, Telangana-500 039.
Email: maheshmokirala@gmail.com

ABSTRACT
Nanotechnology has recently shown great promise in the medical field, which holds great potential for resolving a wide range of medical issues. There are many other types of nanoparticles being researched for potential application as nanomedicines, however Rivea hypocrateriformis (Desr.) stands out. Among the climbing shrubs of the genus Rivea, choisy is among the most tolerant and widespread species in the Indian subcontinent. As a medicinal plant, R. hypocrateriformis has great promise. It has several positive effects on health. The main aim of this research is to characterize the optical, structural, and antibacterial properties of silver nanoparticles prepared from R. hypocrateriformis leaf extract. Synthesizing nanoparticles in a green way has many advantages, including reduced costs, lower environmental impact, and lower toxicity. The techniques like XRD, SEM, FTIR, and UV-vis tests were used to complete the optical and structural characterization. The silver nanoparticles produced from R. hypocrateriformis showed potent antimicrobial activity towards S. aureus, Escherichia coli, and Bacillus subtillis, with a MIC ranging from 20 to 100 g/ml and a MIC-inhibition zone of 2 to 10 millimetres. Against the S. aureus strain, 100 g/ml of silver nanoparticles produced a minimum inhibitory concentration (MIC) of 10 mm. Findings of the present investigation suggest that the produced nanoparticles might be employed as an alternate antibacterial agent for multidrug-resistant bacteria.
Keywords: *Silver nanoparticles, Anti-bacterial activity, Rivera hypocrateriformis, Leaf extracts.*

Received 25.01.2023 Revised 25.02.2023 Accepted 11.03.2023

INTRODUCTION

Nanotechnology is currently the field of manufacturing that is expanding the fastest, and scientists are working feverishly to create new nanomaterials and manufacturing processes. The best examples of nanoscale machines that can carry out a multitude of activities, from energy production to the incredibly efficient extraction of particular materials, are generally acknowledged to be living cells [1].

Where in the many domains, nanotechnology discovers widespread uses is nanomedicine, an innovative key area that was developed as a result of fusing nanotechnology with medicine. Nanoscale materials and devices are employed for pain relief, disease and trauma prevention, diagnosis, treatment, and overall health enhancement, expanding the field of medicine beyond the purview of doctors [2]. Nanotechnology can yield significant insights. For example, clinical approvals have been granted for several treatments based on nanoparticles for treating infections, vaccinations, and kidney disorders [3].

Growing awareness of biological techniques, which produce no environmentally harmful byproducts, has resulted from the pressing need of nontoxic synthetic protocols for nanoparticles creation. "Green nanotechnology" is developing progressively more popular. A broad range of microbes been informed to be used in natural methods for creating nanoparticles, both extracellularly and intracellularly [4]. Due to their lack of hazardous chemicals and abundance of natural topping agents, plants are an ideal nanoparticle synthesis platform. Using plant extracts also decreases the price of isolating and cultivating microorganisms, which makes microbial nanoparticle manufacturing more economically viable [5].

Modern material sciences, nanobiotechnology are where the action is. Because of their unique size, dispersion, and shape, nanoparticles can display a wide range of novel or enhanced features [6]. Human skin, vascular grafts, stainless steel materials, prostheses, dental materials, catheters and all profit from the antimicrobial properties of medical products, including silver used to reduce complications during

burn therapy and surgery [7]. Medicines are just some of the many applications that use silver nanoparticles [8].

Because of their appealing physical and chemical features, silver nanoparticles compete as a crucial part of natural science and medication. Products containing silver have been used for millennia to protect and cure a wide range of ailments, most notably infections, because of their strong repressing and antibacterial properties and the broad range of antimicrobial activity [9].

Medicinal herbs and ancient traditions have been shown to perform an essential part in drug discovery [10], it was evidenced by the discovery and clinical approval of multiple medications through an ethno - medicinal method motivated by knowledge. Additionally, it is simpler and less expensive to find new compounds and create innovative isolation and identifying methods for these plants. There are over 50 genera in the plant family Convolvulaceae, and together they contain close to 1,700 different species [11]. The Convolvulaceae family, of which *R. hypocrateriformis* (Desr.) Choisy is a member responsible for the widespread distribution of this woody climbing shrub, which is found in India, Thailand, Myanmar, Bangladesh, Pakistan, Sri Lanka and Nepal. Malaria, cancer, mental illness, and pain relief are some of the maladies traditionally treated with its bark, stems, and leaves. For example, people from the 1arparkar region of Pakistan have traditionally used this herb to combat malaria and ease discomfort. Antibacterial, anticancer, antioxidant activities are just a few of the many known biological possibilities of the plant. It is also essential to the ayurvedic asthma treatment rasa panchaka [12].

Very little is known about this vital medicinal plant; to our knowledge, no in-depth studies have been conducted on *R. hypocrateriformis* [13]; therefore, the purpose of this paper is to fill that gap by providing a more in-depth analysis of the plant's optical and structural characterization and biological activities. The possible biological effects and antibacterial activity of *R. hypocrateriformis* are also the focus of this research.

MATERIAL AND METHODS

Chemicals and Plant Material Collection

The reagents were the entire analytical grade and were used as is. Around 99.5% pure silver nitrate ($AgNO_3$) (Sigma-Aldrich). For all the tests, aqueous solutions were prepared with distilled water [14].

Preparation of Leaf Extract

Fresh *R. hypocrateriformis* leaves were acquired and rinsed with flowing water to remove dirt or debris. Next, the leaves were rinsed under flowing distilled water to remove any remaining contaminants. Finally, the leaves were ground into a fine powder and used to make aqueous leaf extract. Next, 10 g of the fresh leaves were chopped into bits, weighed, and added to a beaker containing 100 ml of distilled water. After 20 mins of heating at 60°C with periodic mixing, the mixture was cooled to room temperature. After centrifuging the mixture at 5000 rpm for twenty minutes, it was separated through Whatman filter paper. The extract was stored in the refrigerator until further analysis [15].

Synthesis of Ag Nanoparticles

A series of $AgNO_3$ solutions (1 to 5mM) were made by dissolving silver nitrate powder in purified water to make a 10 mM $AgNO_3$ stock solution. In a flask with a volume of 50 mL, the $AgNO_3$ solutions were combined with the aqueous extract of RH leaf extract fresh leaves at a ratio of 1: 1 (v/v). Aluminum foil was used to enclose the flask before being boiled in a water bath at 80 ℃ for 30 minutes.

UV-Visible Absorbance Spectroscopy: 0.5 mL samples were randomly collected from the suspension and examined using a Systronic UV-Visible absorption spectrophotometer 117 and the interaction between metal ions and leaf extract was recorded at 800nm. One hour after application, silver ions reduced, creating silver nanoparticles and$AgNO_3$ stabilized [17].

Fourier Transforms Infrared Spectroscopy (FTIR): The liquid comprising the synthesized silver nanoparticles were centrifuged at 10000 rpm for 30 minutes. The pellet was rinsed three times with 5mL of deionized water to get rid of any extraneous proteins or enzymes that did not engage in encapsulating the silver nanoparticles. Finally, the pellet was dried using a vortex dryer. The FTIR methd was used for the analysis [18].

X-Ray Diffraction: a glass plate was dipped into a solution containing the silver nanoparticles, creating a thin coating. The size of the crystalline silver nanoparticle can be detected by XRD peak width, and the Debye-Scherrer formula may be used to calculate the aggregate dimension of the nanoparticles. [19]:

D= $k\lambda/\ \beta cos\theta$

where D = thickness of the nanocrystal, k = constant, λ = wavelength of X-rays, β = width at half maxima of reflection at Bragg's angle 2θ, and θ = Bragg angle. The Debye-Scherrer formula was used to calculate the size of the silver nanoparticle by analyzing the line broadening of the reflection. Corresponding to the principle, constant (k) = 0.94 and wavelength (λ) = 1.5406 × 10 −10.

Scanning Electron Microscopy: For SEM analysis, we created thin films of the sample by depositing a tiny bit of the material onto a carbon-coated copper grid, removing any excess liquid with absorbent paper, and then drying the film.

Assay for Antibacterial Activity of Ag Nanoparticles:

Using agar disc diffusion and microdilution plate techniques, the antibacterial activity of silver nanoparticles nanoparticles synthesized by *R. hypocrateriformis* was studied against isolates of *Bacillus cereus*, *E. coli*, and *S. aureus*. Cultures of bacteria, including *E. coli* MTCC 424, *Staphylococcus aureus* MTCC 96, and *Bacillus subtillis* MTCC 3053, are dispersed on nutrient agar plates. After the samples have been activated, they are deposited using the proper procedure and left to incubate for a full day. After incubation for 24 hours, a distinct zone of bacterial inhibition was identified surrounding the sample and assessed. Anti-bacterial activity-displaying samples are employed in follow-up research.

Characterization of Ag Nanoparticles:

In order to see the degradation of pure Ag+ ions, the UV-Vis spectra of the response method was used after reducing a tiny aliquot part of the test with purified water. In addition, the reaction combination (metal ion solution + RH extract) was visually observed by change in colour. The UV-Vis spectral analysis was performed at 200-800 nm range using a UV-Vis spectrophotometer UV-1800 (Shimadzu). In addition, the Litesizer 500, a particle size measuring instrument (DLS) The form and size of Ag nanoparticles were analyzed using particle size distribution by the intensity and Particle size distribution peaks [20].

RESULTS

Plant profile

Classification of *Riveahypocrateriformis*

Kingdom	**Plante**
Phylum	**Tracheophyta**
Class	**Magnoliopsida**
Subclass	**Asteridae**
Order	**Solanales**
Family	**Convolvulaceae**
Genus	***Rivea***
Species	***hypocrateriformis***

Morphology of *R.hypocrateriformis*

Morphological characterization of the *R. hypocrateriformis* plant and its parts are presented in (Figures1A&B). Leaves are round-heart-shaped, blunt apically, densely appressed velvet-hairy below. Its flowers, usually solitary, are creamy white, typical morning glory form, flat-faced, and 6–9 cm long. Sepals unequal, ovate, blunt apically, 10–12 mm long with dense short villoses. Fruit are indehiscent or tardily dehiscent, dry-baccate of 2 cm long. Seeds are brown, smooth, glabrous, slightly trigonous, and surrounded by a dry white pulp.

A B

Fig-1A:*R. Hypocrateriformis* Plant with leaf with flower;1B: Plant with with fruit

UV-Vis Spectra Analysis

When the aqueous extract of fresh RH leaves is heated, it undergoes a metamorphic colour shift. Colorless RH extract turns a brownish hue upon further processing (Figure.1).

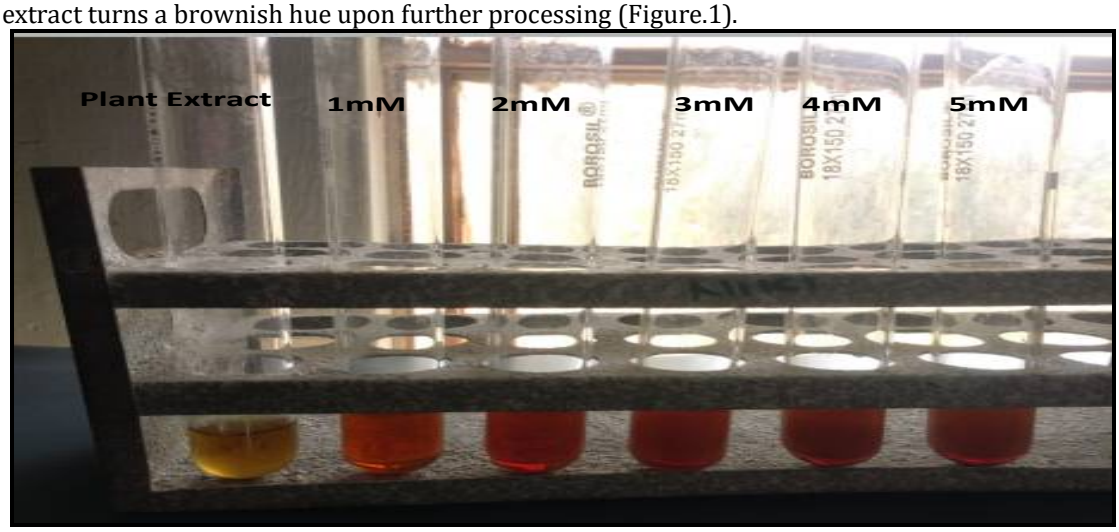

Figure.2. Synthesis of silver nanoparticles using *RH* fresh leaf extract.

After adding the $AgNO_3$ solution, the colour of this warm extract solution changed one more time. When the temperature rises, some of the silver ions are decreased, giving rise to the Ag+ complex that causes the colour shift. The extract of RH changed from a brownish yellow to a greyish brown due to the presence of this complex. The production of Ag nanoparticles is represented by this shift in hue. UV-Vis spectroscopy was used to study the Ag nanoparticles generated in each extract solution. For this purpose, Ag nanoparticles were produced at varying levels of $AgNO_3$ (from 1 mM to 5 mM) to analyse their peak spectra (Figure 1).

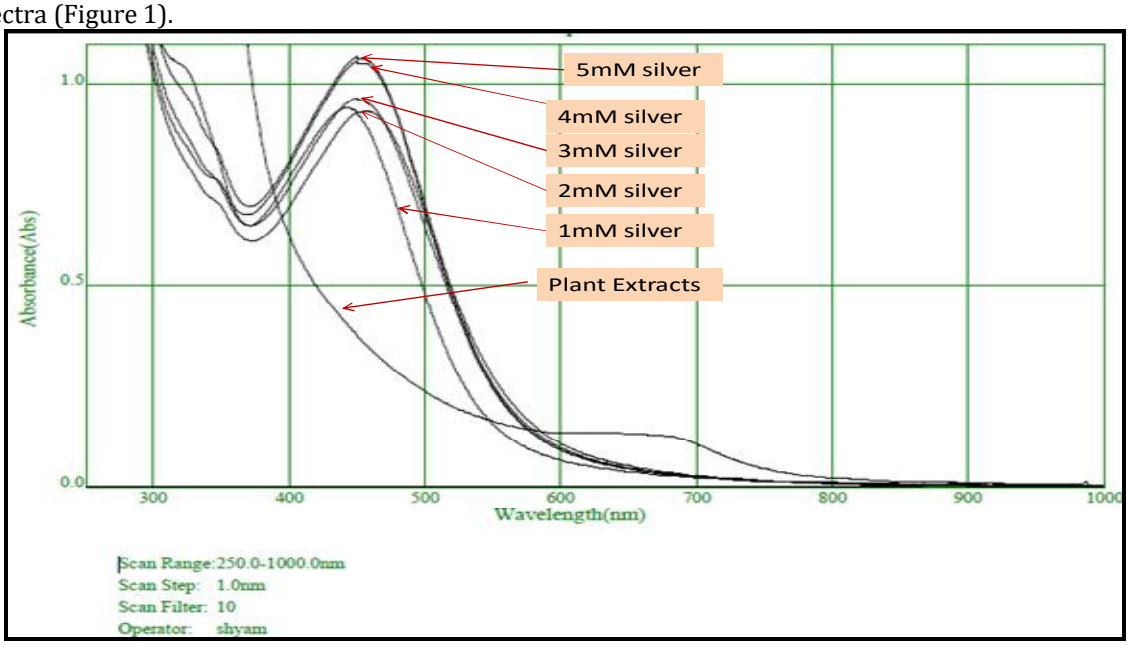

Figure.3. UV-VIS spectroscopy for silver nanoparticles synthesized using *RH* leaves extracts and different silver nitrate concentrations.

Normal Silver nanoparticle properties are seen between 250 and 1000 nm. The blue shift of the maximum absorption is visible in the UV-Vis spectra of silver nanoparticles produced using the leaf extract. The absorption peak is located at 450-420 nm for 5 samples from 1 to 5mM samples, respectively. This data demonstrates the creation of Ag nanoparticles in the isolate, where silver ions have been converted to silver oxide. In the decreasing and capping mechanisms of nanoparticle production [21], all secondary metabolites of the isolate perform a crucial role. Similar behaviors are shown in the silver nanoparticles found in the RH extract's aqueous extract, such as the absorption band shift with increasing $AgNO_3$ concentrations.

Silver nanoparticles produced from RH leaf extracts have a UV-VIS absorption spectrum, as shown in Figure 2. The absorption peak between 352 nm and 368 nm found for RH leaf extracts of 1 mM-5 mM is

due to the photoexcitation of electrons from the valence band into the excitons (Figure 2). Near-band edge emissions at 352-368nm have been seen in nanoparticles extracted from RH leaves, which may result from confined or free excitons based on the band-to-band recombination mechanism [22]. Absorption spectra in the UV-VIS range for RH-silver nanoparticles are displayed in Figure 2. The surface plasmon resonance effect caused a significant reduction in the transmission of electromagnetic waves in the visual range by nanoparticles. The highest wavelength at 368nm was observed in UV-VIS spectra, indicating successful nanoparticle production and a spherical particle morphology [23]. The UV-VIS spectrum confirmed the silver nanoparticles' efficiency in production. A similar spectrum was reproduced by other scientists [24], so we know it's accurate. The UV-VIS spectra in Figure 1 also show only one absorption nanoparticle band, suggesting that the particles likely have an uneven size dispersion [25].

FTIR Analysis:

The proteins that may have capped and effectively stabilized the silver nanoparticles generated by the leaf extracts were investigated using FTIR. The RH leaf extract is shown in Figure 3. RH silver nano exhibited absorbance bands at 3336.96 cm1 assigned to O-H (s) stretch, 1672.34 cm1 assigned to C=C aromatic stretch, 1398.44 cm1 attributed to C-H alkenes stretch, 1186.26 cm1 assigned to C-N amines stretch, and 719.46 cm1 and 669.32 cm1 assigned to C-H alkenes stretch.

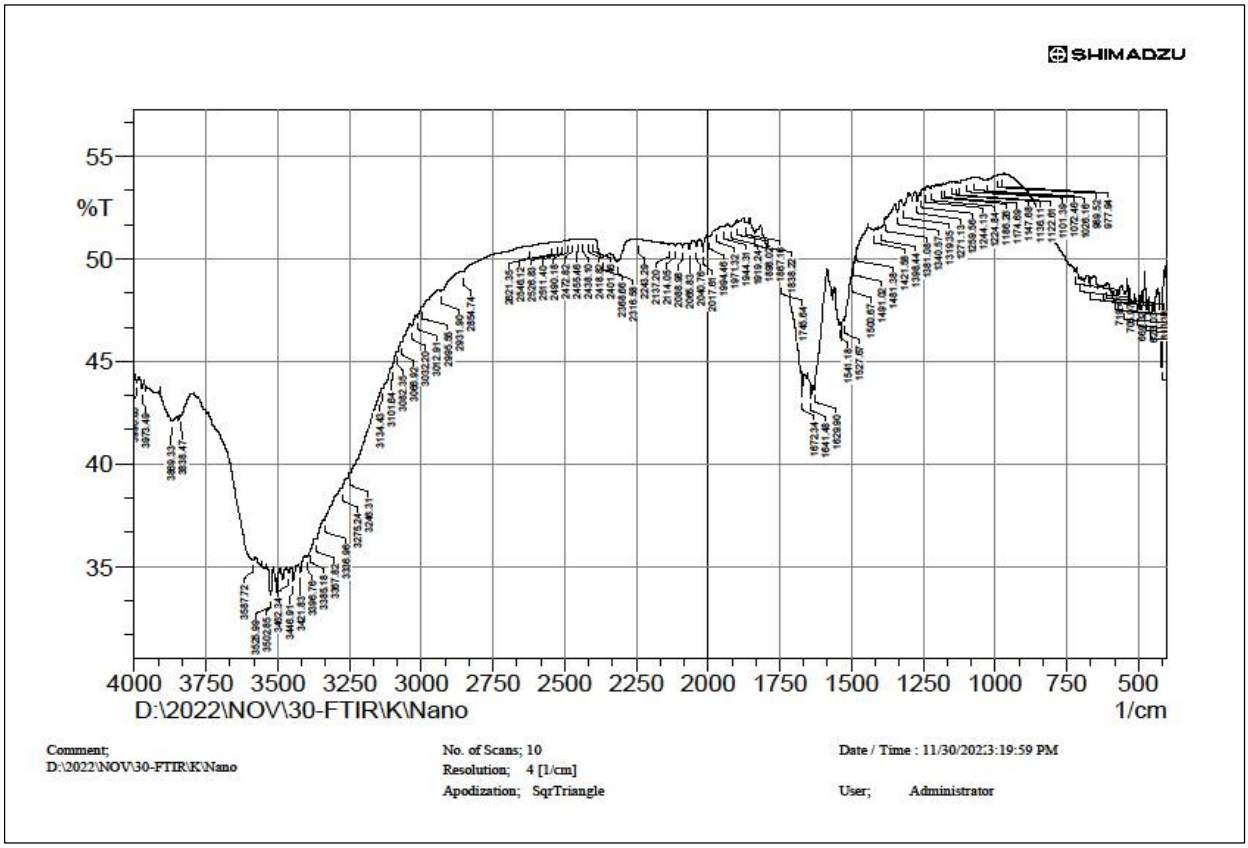

Fig -4 FTIR analysis of *R. hypocrateriformis*leaf

The FTIR spectra of silver nanoparticles in R.*hypocrateriformis* are shown in Figure 3. Typical FTIR bands of silver nanoparticles were observed in the RH at 1672.34 cm1, 1398.44 cm1, and 1186.26 cm1 (all assigned to CH curvature modes from -CH_2), indicating stretching, bending, and deflection, respectively, in the carbonyl group of the pyrrolidone ring. The -OH stretching vibration is also associated with the 3336.96 cm1 broadband [26]. In the spectra of $AgNO_3$ (trace B), there were many peaks at 3430.00, 2082.50, and 1633.52 cm1. However, the carbonyl peak of PVP was found to be displaced from 1634.52 to 1636.30 after silver reduction during the synthesis of silver Nanoparticles-PVP. Other researchers have also noticed similar changes [26], The absence of the $AgNO_3$ peaks and coexistence of the PVP peaks in the spectra of silver Nanoparticles-PVP (trace C), verified the reduction and coating of silver with PVP and the production of silver Nanoparticles polymers. Other studies have also seen the lack of $AgNO_3$ peaks in silver Nanoparticles and have drawn the same conclusion that the reduction of silver ions is connected to the decrease of capped materials [27].

Scanning Electron Microscope (SEM) Analysis:

SEM is an analytic tool for direct surface imaging that can distinguish between nanoparticles of varying sizes, shapes, and surface morphogenesis. When the *R. hypocrateriformis* silver nanoparticles have dried, they are coated in conductive metal using a sputter coater in an ultravacuum environment. Then, an intense electron beam is used in SEM to create a three-dimensional model of the particle [28].

The SEM picture of the silver nanoparticles in *RH* is shown in Figure 4. Silver nanoparticles are found on the cell surface in a somewhat even distribution. Nevertheless, this does not prove that all silver nanoparticles are attached to the cells; some may have been dispersed in the fluid and deposited on the cells during drying before SEM could be performed. Sizes of spherical nanoparticles in this SEM image were measured to be 93.5nm, 103nm, 109nm, 112nm, 114nm, 120nm, 122nm, 125nm, and 148nm. Silver nanoparticles created in the lab have been measured at 159 nm and 169 nm in size and have been seen to exhibit a wide range of morphologies. Leaf extracts from *Musa balbisiana*, *Azadirachta indica*, and *Ocimumtenuiflorum* were used in the synthesis of *R.hypocrateriformis*nanoparticles [29], with the resulting particles taking on a roughly spherical, triangular, and cuboidal shape, accordingly. As expected, spherical nanoparticles were formed during the production of silver nanoparticles using an aqueous extract of *Rosa brunonii* [30].

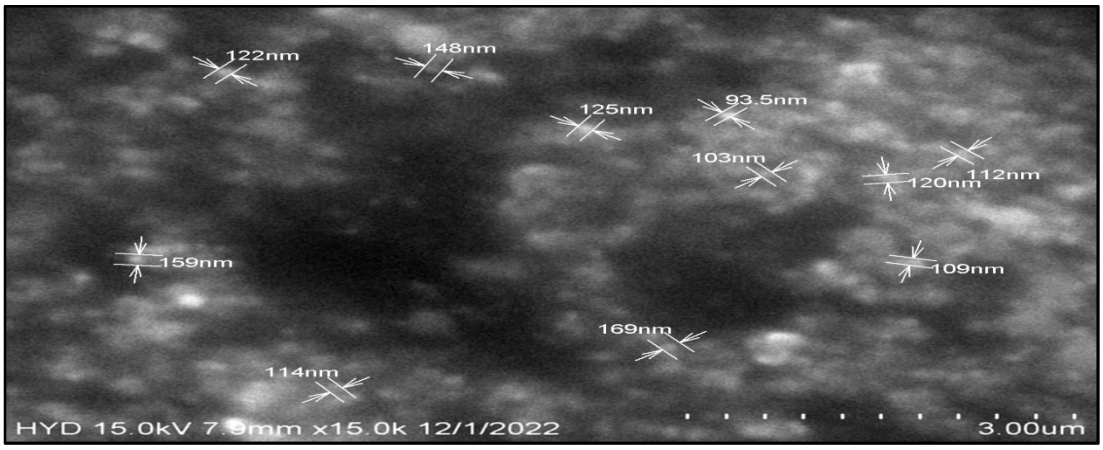

Figure.5: SEM micrograph of silver nanoparticles synthesized by using the leaf extract of *RH extracts*

The silver nanoparticles' size was measured using dynamic light scattering (DLS) techniques. The size variation of the produced silver nanoparticles is depicted in (Figure.5 and 6). DLS is used to determine particle size and distribution by evaluating the particles' rotation and translation diffusion coefficients. Colloidal suspensions with Brownian particles can have their sizes determined by this method. While shining monochromatic light on an RH solution of silver nanoparticles, the particles' sizes were seen to range from 14.5 nm to 310 nm, with an average particle size of 63.5 nm. The size variation of silver nanoparticles was also quite narrow, with a variation of only 63.5 nm between the largest and smallest particles [31].

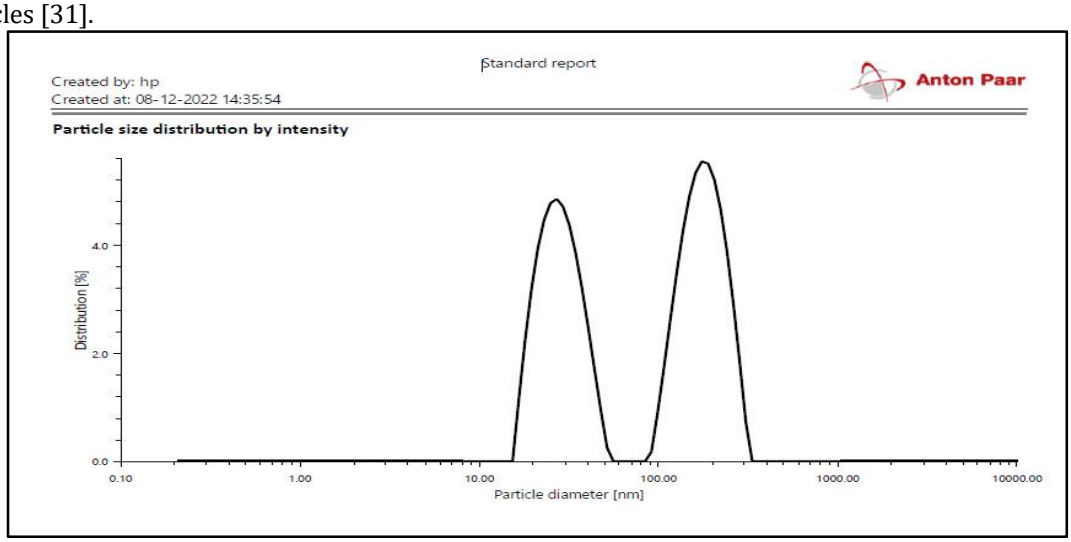

Figure.6: Particle size curve for silver nanoparticles synthesized using the leaf extract of RH leaf powder.

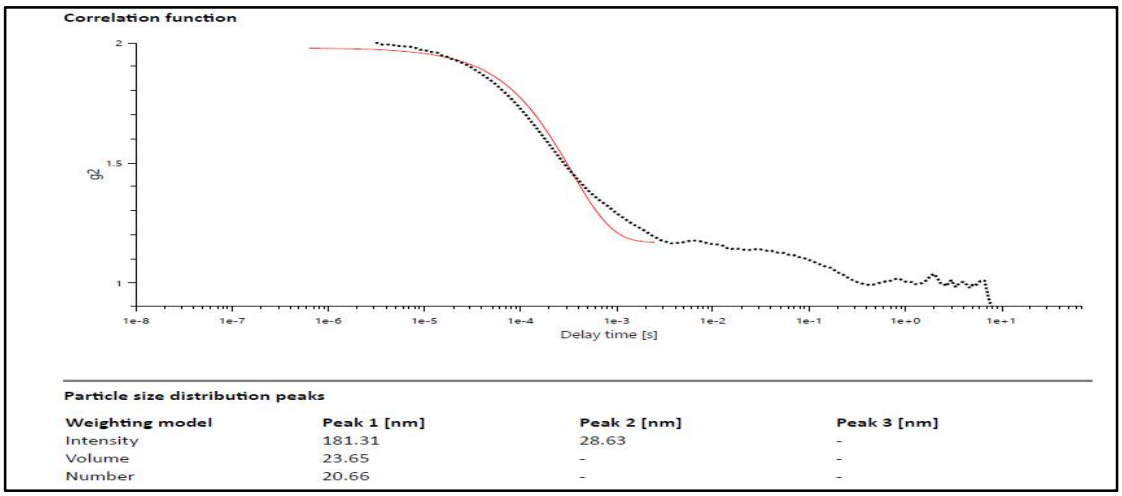

Figure.7: Particle size distribution curve for silver nanoparticles synthesized using the leaf extract of RH leaf powder.

The nanoparticles' sustainability, as determined by their zeta potential, was also calculated to be -58.4 mV (Figure.7). The negative value suggested the nanoparticles were stable and could avoid clumping together [32]. After colliding with the moving particles, the entering beam of light undergoes a Doppler shift and a wavelength shift proportional to the particle size and distribution. DLS study validated the 39-78.5nm size of silver nanoparticles synthesized using liquid extract of Chamaemelum nubile [33].

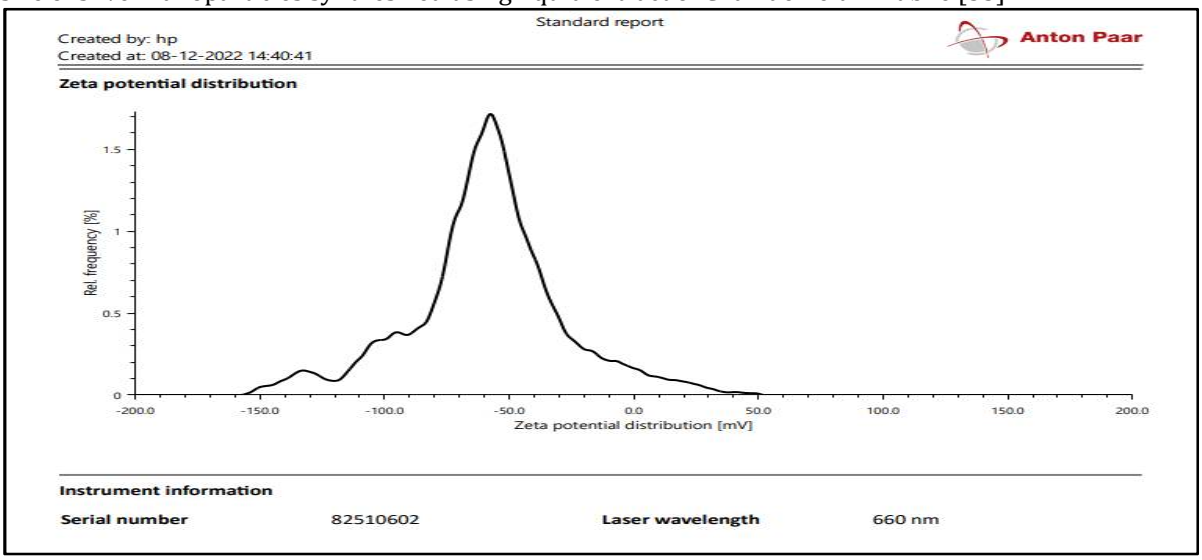

Figure.8: Zeta Potential analysis of AgNps prepared of RH leaf extract

X-ray diffraction (XRD) analysis:

The nanoparticles' crystallographic properties can be determined by XRD, a quasi analytical methodology. Nanoparticle analysis is based on diffraction patterns, which are formed based on the particle's size and crystal shape. Distinct peaks at 2 values were seen in the XRD pattern; their corresponding angles (intensities) range from 25.603 to 28.388, 32.170 to 40.390, 44.352 to 64.534 to 77.510 to 82.331. (table 1). To the 111, 200, 220, and 311 crystalline planes of silver nanoparticles (Figure.8). A face-centered cubic lattice is linked to these peaks. The organic residue of the plant extract accounts for the additional peaks at 2θ values in the nanoparticle design. Some plant metabolite subunits crystallized atop the silver nanoparticles, as shown by the peaks.

This is a valid indication that the chemical components of plant extracts played a role in creating silver nanoparticles. The secondary metabolites are indisputable in biosynthesis, while the precise mechanism of the biosynthesis method by plant extract is unknown. Extracts of RH species have been shown to contain the carboxylate-containing compounds carnosic acid and flavonoids. These metabolites interact with silver ions, leading to the bioreduction of silver nitrate and the production of silver nanoparticles. Carboxylate (COO) and polar groups like hydroxyl (OH) and carbon monoxide (CO) are examples of

negatively charged compounds found in plant extracts that have a strong affinity for attaching to Ag^{+}. Hence, these compounds assist the decrease and stability of Silver ions. It has been hypothesized that carnosic acid, flavonoids, and proteins play a significant part in the potential process for bio decline of silver ions [34], as do other plant metabolites comprising OH, CO, and particularly COO.

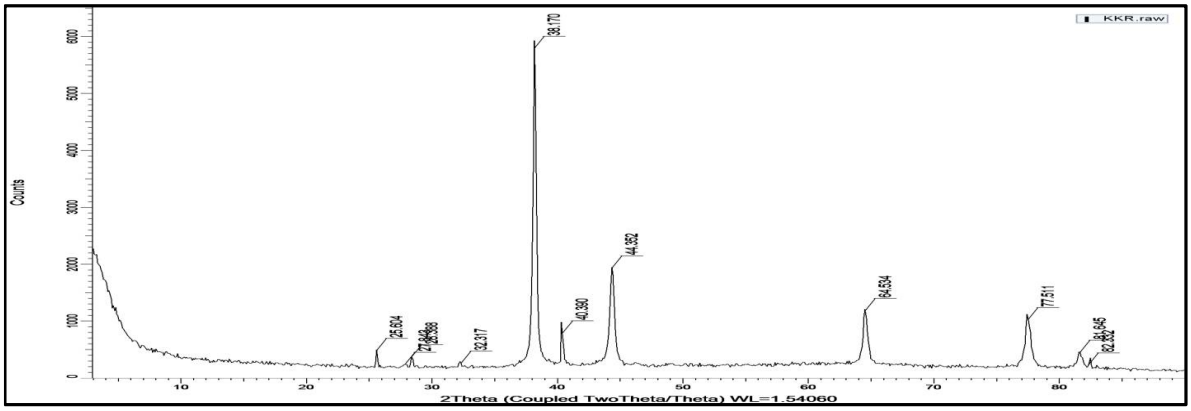

Figure.9 :X-ray diffraction profile from dried silver nanoparticles biosynthesized by RH extracts

The cell volume, lattice constants, and d-spacing measurements validate the crystalline nature of the greenly produced nanoparticles. The Debye-Scherrer equation [35] extrapolates a particle's average crystallinity size from an XRD spectrum. Broad XRD peaks indicate the crystallinity and reduced size of the silver nanoparticles. Based on XRD examination, the average crystalline size of Ag NPs generated using ethanolic Santalum album fruit extract is estimated to be 20nm [36].

The nanoparticles' crystallographic properties can be determined by X-ray diffraction (XRD), a non-destructive analytical method. Nanoparticle analysis is based on diffraction patterns formed based on the particle's size and crystal structure.

Table 1: XRD pattern revealed distinct peaks at 2θ values calculation.

Index	Angle	d Value	Net Intensity	Gross Intensity	Rel. Intensity
1	25.60385	3.476377	290.258	485.3649	0.052566
2	27.84261	3.201726	47.37631	241.9843	0.00858
3	28.38818	3.141423	179.9145	373.3304	0.032583
4	32.31677	2.767941	69.37617	261.4887	0.012564
5	38.1702	2.355858	5521.795	5790.587	1
6	40.39021	2.231344	530.0918	789.5554	0.096
7	44.35246	2.040764	1664.67	1931.355	0.301473
8	64.5343	1.442867	905.9789	1186.258	0.164073
9	77.51088	1.230516	801.6976	1026.108	0.145188
10	81.64471	1.178341	254.864	452.8097	0.046156
11	82.33199	1.170237	37.6676	232.1383	0.006822

Antibacterial Activity:

Microbes toxic effects are triggered by silver ions, Silver nanoparticles, and manufactured nanoparticles loaded with other substances. Positive antibacterial activity against *Escherichia coli*, *Bacillus cereus*, and *Staphylococcus aureus* were observed in silver nanoparticles produced using RH. When attached to an active group of proteins, silver nanoparticles cause protein decomposition or impede genetic material multiplication [37]. This gives silver nanoparticles antibacterial abilities.Leaf extract of the plant *R. hypocrateriformis* have been demonstrated to facilitate the synthesis of spherical silver nanoparticles with a maximum size of 10 mm at a concentration of 100 g/ml. Against *Escherichia coli*, *Bacillus cereus*, and *Staphylococcus aureus*, a MIC of 100 g/ml was optimal, with a maximal inhibition zone of 9, 9, and 10mm, respectively. Bioactive chemicals acting as stabilizing agents/capping agents on the surface of nanoparticles were responsible for their increased antibacterial activity [38].

Table:2 antibacterial activity of *R. Hypocrateriformis* leaf extract

S. No	Concentration silver nanoparticles biosynthesized by *R.hypocrateriformis* extracts	*E. coli*	*B. cereus*	*S. aureus*
1	20 µg/ml	3mm	2mm	3mm
2	40 µg/ml	5mm	4mm	4mm
3	60 µg/ml	6mm	6mm	6mm
4	80 µg/ml	8mm	8mm	7mm
5	100 µg/ml	9mm	9mm	10mm

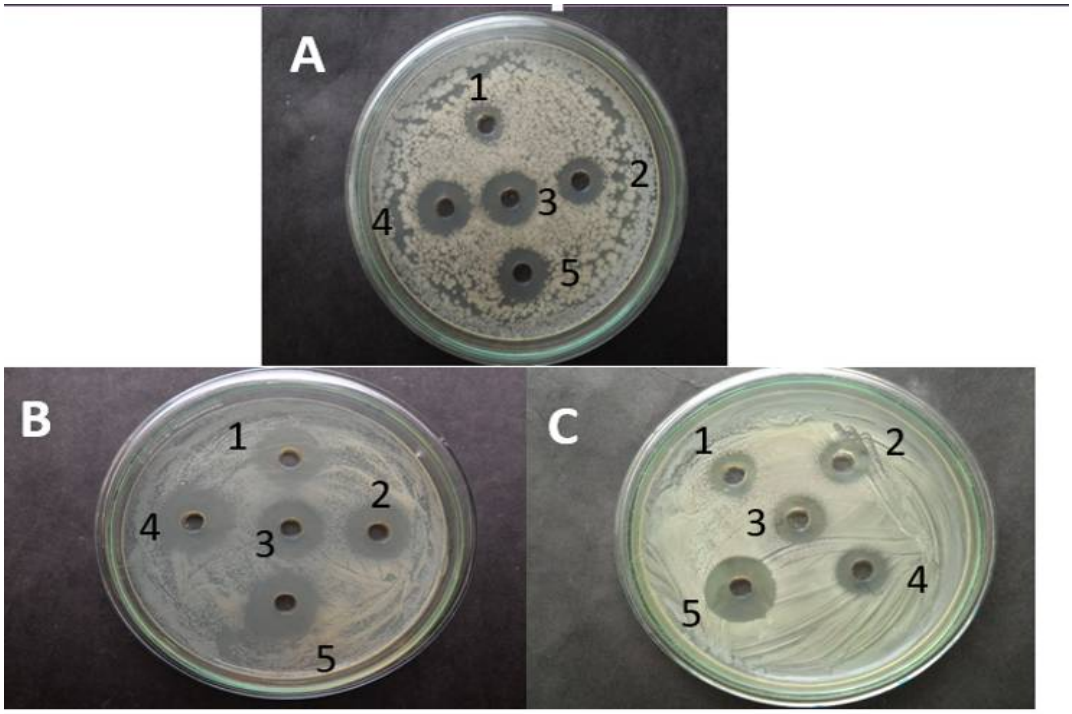

A: *Bacillus cereus* B: *E.coli* C: *S. aureus*

Fig.10:Here 1 to 5 is the concentration of silver nanoparticles biosynthesized by *R. hypocrateriformis* extracts

At a 100 mg/ml dose of silver nanoparticles, it was revealed that *S. aureus* had the biggest zone of inhibition (10 mm), whereas *E. coli* and *Bacillus cereus* had the smallest (9 mm). This study's findings are consistent with those of Jyoti et al. [39]. While no zone of inhibition was found in the produced Au nanoparticles, this research concludes that Au nanoparticles had no toxic effect on multidrug-resistant bacteria. High concentrations of Au nanoparticles against multidrug resistant did not kill the bacteria. In vitro, the highest minimum inhibition concentration of Au nanoparticles against *P. aeruginosa* strains was 114 mg/ml. [38].

CONCLUSIONS

Green technology for the rapid production of silver nanoparticles has been established, and this study provides a novel way of dealing with antibacterial activity by employing extract from the leaves of the *R. hypocrateriformis* plant. According to FT-IR research and the zeta potential value, silver nanoparticles were produced at a wavelength of 368 nm, as determined by UV-Vis spectroscopic examination. Unlike when kept at higher temperatures, the physical properties of *R. hypocrateriformis* silver nanoparticles are maintained even when the temperature is lowered. The RH silver nanoparticles generated were found to be of the Face-Centered Cubic (FCC) phase, according to the XRD examination. Particles are spherical or hexagonal with a limited size distribution of 111-311 nm under ideal circumstances. The biological ability of RH silver nanoparticles to prevent bacterial growth was also shown to be higher than that of other nanoparticles studied. *R. hypocrateriformis* considered to be a potential medicinal herb with a wide range of therapeutic and health-promoting qualities, as evidenced by the present study's discoveries that highlight the traditional usages and pharmacological activity of its extracts and components.

ACKNOWLEDGEMENT
The authors are thankful to Prof. B. Rama Devi, Head, Department of Botany, Osmania University Hyderabad for providing facilities and encouragement, and also authors thankful to the Department of Physics Osmania University Hyderabad for providing SEM and XRD facilities

Conflict of interest: None.

REFERENCES

1. M. Saravanan, B. Hamed, V. Hossein et al.,(2021). "Emerging theranostic silver and gold nanobiomaterials for breast cancer: present status and future prospects," in *Handbook on Nanobiomaterials for Derapeutics and Diagnostic Applications*, pp. 439–456, Elsevier, Amsterdam, Netherlands.
2. D. Roe, B. Karandikar, N. Bonn-Savage, B. Gibbins, and J. B. Roullet, (2008). "Antimicrobial surface functionalization of plastic catheters by silver nanoparticles," *Journal of Antimicrobial Chemotherapy*, vol. 61, no. 4, pp. 869–876.
3. C. Pansara, W. Y. Chan, A. Parikh et al., (2019). "Formulation optimization of chitosan-stabilized silver nanoparticles using in vitro antimicrobial assay," *Journal of Pharmaceutical Sciences*, vol. 108, no. 2, pp. 1007–1016, 2019.
4. H. Barabadi, H. Vahidi, K. DamavandiKamali et al., (2020). "Emerging theranostic silver nanomaterials to combat colorectal cancer: a systematic review," *Journal of Cluster Science*, vol. 31, no. 2, pp. 311–321.
5. M. Ayaz, F. Ullah, A. Sadiq, M. O. Kim, and T. Ali, (2019). "Editorial: natural products-based drugs: potential therapeutics against Alzheimer's disease and other neurological disorders," *Frontiers in Pharmacology*, vol. 10, p. 1417.
6. M. Ovais, M. Ayaz, A. T. Khalil et al., (2018). "HPLC-DAD finger printing, antioxidant, cholinesterase, and α-glucosidase inhibitory potentials of a novel plant olax nana," *BMC Complementary and Alternative Medicine*, vol. 18, no. 1, p. 1, 12-18.
7. C. Govil, (1972). "Morphological studies in the family convolvulaceae," *Proceedings of the Indian Academy of Sciences-Section B*, vol. 75, pp. 271–282.
8. D. J. Mabberley, (1997). *Plant-Book: A Portable Dictionary of the Vascular Plants*, Cambridge University Press, Cambridge, MA, USA.
9. B. Salehi, B. Krochmal-Marczak, D. Skiba et al.,(2020). "Convolvulus plant—a comprehensive review from phytochemical composition to pharmacy," *Phytotherapy Research*, vol. 34, no. 2, pp. 315–328.
10. B. N. Dhawan, M. P. Dubey, B. N. Mehrotra, R. P. Rastogi, and J. S. Tandon, (1980). "Screening of Indian plants for biological activity: part IX," *Indian Journal of Experimental Biology*, vol. 18, no. 6, pp. 594–606.
11. A. H. Abdellatif, M. Alsharidah, O. Al Rugaie, H. M. Tawfeek, and N. S. Tolba, (2021). "Silver nanoparticle-coated ethyl cellulose inhibits tumor necrosis factor-alpha of breast cancer cells," *Drug Design, Development and Derapy*, vol. 15, pp. 2035–2046.
12. R. Bryaskova, D. Pencheva, S. Nikolov, and T. Kantardjiev, (2011). "Synthesis and comparative study on the antimicrobial activity of hybrid materials based on silver nanoparticles (AgNps) stabilized by polyvinylpyrrolidone (PVP)," *Journal of Chemistry Biology*, vol. 4, no. 4, pp. 185–191.
13. S. Hajji, R. B. S. B. Salem, M. Hamdi et al., (2017). "Nanocomposite films based on chitosan-poly(vinyl alcohol) and silver nanoparticles with high antibacterial and antioxidant activities," *Process Safety and Environmental Protection*, vol. 111, pp. 112–121.
14. S. Pal, Y. K. Tak, and J. M. Song, (2007). "Does the antibacterial activity of silver nanoparticles depend on the shape of the nanoparticle? a study of the Gram-negative bacterium *Escherichia coli*," *Applied and Environmental Microbiology*, vol. 73, no. 6, pp. 1712–1720.
15. S. Mahmood, U. K. Mandal, B. Chatterjee, and M. Taher,(2017). "Advanced characterizations of nanoparticles for drug delivery: investigating their properties through the techniques used in their evaluations," *Nanotechnology Reviews*, vol. 6, no. 4, pp. 355–372.
16. P. Banerjee, M. Satapathy, A. Mukhopahayay, and P. Das, (2014). "Leaf extract mediated green synthesis of silver nanoparticles from widely available Indian plants: synthesis, characterization, antimicrobial property and toxicity analysis," *Bioresources and Bioprocessing*, vol. 1, no. 1, p. 3.
17. M. Bhagat, R. Anand, R. Datt, V. Gupta, and S. Arya, (2019). "Green synthesis of silver nanoparticles using aqueous extract of *Rosa brunonii*Lindl and their morphological, biological and photocatalytic characterizations," *Journal of Inorganic and Organometallic Polymers and Materials*, vol. 29, no. 3, pp. 1039–1047.
18. Alahmad, A. Feldhoff, N. C. Bigall, P. Rusch, T. Scheper, and J.-G. Walter,(2021). "*Hypericum perforatum*L.-mediated green synthesis of silver nanoparticles exhibiting antioxidant and anticancer activities," *Nanomaterials*, vol. 11, no. 2, Article ID 487.
19. K. Keshari, R. Srivastava, P. Singh, V. B. Yadav, and G. Nath,(2020). "Antioxidant and antibacterial activity of silver nanoparticles synthesized by *Cestrum nocturnum*," *Journal of Ayurveda and Integrative Medicine*, vol. 11, no. 1, pp. 37–44.
20. T. Dutta, N. N. Ghosh, M. Das, R. Adhikary, V. Mandal, and A. P. Chattopadhyay, (2020). "Green synthesis of antibacterial and antifungal silver nanoparticles using *Citrus limetta* peel extract: experimental and theoretical studies," *Journal of Environmental Chemical Engineering*, vol. 8, no. 4, Article ID 104019.

21. M. R. Bindhu, M. Umadevi, G. A. Esmail, N. A. Al-Dhabi, and M. V. Arasu, (2020). "Green synthesis and characterization of silver nanoparticles from *Moringa oleifera* flower and assessment of antimicrobial and sensing properties," *Journal of Photochemistry and Photobiology B: Biology*, vol. 205, ArticleID 111836.
22. Nouri, M. TavakkoliYaraki, A. Lajevardi, Z. Rezaei, M. Ghorbanpour, and M. Tanzifi, (2020). "Ultrasonic-assisted green synthesis of silver nanoparticles using *Mentha aquatica* leaf extract for enhanced antibacterial properties and catalytic activity," *Colloid and Interface Science Communications*, vol. 35, 109-111.
23. M. N. Lakhan, R. Chen, A. H. Shar et al., (2020). "Eco-friendly green synthesis of clove buds extract functionalized silver nanoparticles and evaluation of antibacterial and antidiatom activity," *Journal of Microbiological Methods*, vol. 173, Article ID 105934.
24. M. Maghimaa and S. A. Alharbi, (2020). "Green synthesis of silver nanoparticles from *Curcuma longa* L. and coating on the cotton fabrics for antimicrobial applications and wound healing activity," *Journal of Photochemistry and Photobiology B: Biology*, vol. 204, Article ID 111806.
25. M. Devi, S. Devi, V. Sharma, N. Rana, R. K. Bhatia, and A. K. Bhatt, (2020). "Green synthesis of silver nanoparticles using methanolic fruit extract of *Aegle marmelos*and their antimicrobial potential against human bacterial pathogens," *Journal of Traditional and Complementary Medicine*, vol. 10, no. 2, pp. 158–165.
26. S. Choudhary, R. Kumar, U. Dalal, S. Tomar, and S. N. Reddy, (2020). "Green synthesis of nanometal impregnated biomass-antiviral potential," *Materials Science and Engineering: C*, vol. 112, Article ID 110934.
27. N. Anwar, A. Khan, M. Shah et al., (2022). "Hybridization of green synthesized silver nanoparticles with poly(ethylene glycol) methacrylate and their biomedical applications," *PeerJ*, vol. 10, Article ID e12540.
28. Y. Huang, C. Y. Haw, Z. Zheng, J. Kang, J. C. Zheng, and H. Q. Wang, (2021). "Biosynthesis of zinc oxide nanomaterials from plant extracts and future green prospects: a topical review," *Advanced Sustainable Systems*, vol. 5, no. 6, Article ID 2000266.
29. J. S. Kim, E. Kuk, K. N. Yu et al.,(2007). "Antimicrobial effects of silver nanoparticles," *Nanomedicine: Nanotechnology, Biology and Medicine*, vol. 3, no. 1, pp. 95–101.
30. G. Madhumitha, G. Elango, and S. M. Roopan, (2015). "Bio-functionalized doped silver nanoparticles and its antimicrobial studies," *Journal of Sol-Gel Science and Technology*, vol. 73,no. 2, pp. 476–483.
31. M. Bilal, T. Rasheed, H. M. N. Iqbal, H. Hu, and X. Zhang, (2017)."Silver nanoparticles: biosynthesis and antimicrobial potentialities," *International Journal of Pharmacology*, vol. 13, no. 7, pp. 832–845.
32. K. Keshari, R. Srivastava, P. Singh, V. B. Yadav, and G. Nath, (2020). "Antioxidant and antibacterial activity of silver nanoparticles synthesized by *Cestrum nocturnum*," *Journal of Ayurveda and Integrative Medicine*, vol. 11, no. 1, pp. 37–44.
33. N. Sisubalan, C. Karthikeyan, V. S. Senthil Kumar et al.,(2021). "Biocidal activity of Ba2+-doped CeO2 NPs against streptococcus mutans and *Staphylococcus aureus* bacterial strains," *RSC Advances*, vol. 11, no. 49, pp. 30623–30634.
34. Fernandes IJ, Aroche AF, Schuck A, Lamberty P, Peter CR, Hasenkamp W, *et al.* (2020). Silver nanoparticle conductive inks: Synthesis, characterization, and fabrication of inkjet-printed flexible electrodes. Sci Rep ;10(1):1-11.
35. Asiya SI, Pal K, Kralj S, El-Sayyad GS, de Souza FG, Narayanan T. (2020). Sustainable preparation of gold nanoparticles *via* green chemistry approach for biogenic applications. Mater Today Chem;17:100327.
36. Maria BS, Devadiga A, Shetty Kodialbail V, Saidutta MB. (2015). Synthesis of silver nanoparticles using medicinal *Zizyphusxylopyrus*bark extract. ApplNanosci;5(6):755-62.
37. Kabra, R. Sharma, C. Hano, R. Kabra, N. Martins, and U. S. Baghel,(2019). "Phytochemical composition, antioxidant, and antimicrobial attributes of different solvent extracts from myrica esculenta buch.-ham. ex. D. don leaves," *Biomolecules*, vol. 9, no. 8, p. 357.
38. M. Ayaz, F. Ullah, A. Sadiq et al., (2019). "Synergistic interactions of phytochemicals with antimicrobial agents: potential strategy to counteract drug resistance," *Chemico-Biological Interactions*, vol. 308, pp. 294–303.
39. Ajitha, B., Reddy, Y.A.K., Reddy, P.S.: (2014). Biogenic nano-scale silver particles by Tephrosia purpurea leaf extract and their inborn antimicrobial activity. Spectrochimica Acta, Part A 121, 164–172.

CITATION OF THIS ARTICLE

M.Mahesh, G.Prabhakar and P. Kamalakar. Studies on Silver Nanoparticle Preparation, Synthesis, and Anti-Bacterial Activity of *Rivea hypocrateriformis* (Desr.) Choisy. Bull. Env.Pharmacol. Life Sci., Vol 12 [4] March 2023: 161-171